NASA/TM–2011-217145

A Data System for a Rapid Evaluation Class of Subscale Aerial Vehicle

Edward F. Hogge
Lockheed Martin, Hampton, Virginia

Cuong C. Quach and Sixto L. Vazquez
Langley Research Center, Hampton, Virginia

Boyd L. Hill
Vigyan Inc., Hampton, Virginia

May 2011

NASA STI Program . . . in Profile

Since its founding, NASA has been dedicated to the advancement of aeronautics and space science. The NASA scientific and technical information (STI) program plays a key part in helping NASA maintain this important role.

The NASA STI program operates under the auspices of the Agency Chief Information Officer. It collects, organizes, provides for archiving, and disseminates NASA's STI. The NASA STI program provides access to the NASA Aeronautics and Space Database and its public interface, the NASA Technical Report Server, thus providing one of the largest collections of aeronautical and space science STI in the world. Results are published in both non-NASA channels and by NASA in the NASA STI Report Series, which includes the following report types:

- TECHNICAL PUBLICATION. Reports of completed research or a major significant phase of research that present the results of NASA programs and include extensive data or theoretical analysis. Includes compilations of significant scientific and technical data and information deemed to be of continuing reference value. NASA counterpart of peer-reviewed formal professional papers, but having less stringent limitations on manuscript length and extent of graphic presentations.

- TECHNICAL MEMORANDUM. Scientific and technical findings that are preliminary or of specialized interest, e.g., quick release reports, working papers, and bibliographies that contain minimal annotation. Does not contain extensive analysis.

- CONTRACTOR REPORT. Scientific and technical findings by NASA-sponsored contractors and grantees.

- CONFERENCE PUBLICATION. Collected papers from scientific and technical conferences, symposia, seminars, or other meetings sponsored or co-sponsored by NASA.

- SPECIAL PUBLICATION. Scientific, technical, or historical information from NASA programs, projects, and missions, often concerned with subjects having substantial public interest.

- TECHNICAL TRANSLATION. English-language translations of foreign scientific and technical material pertinent to NASA's mission.

Specialized services also include creating custom thesauri, building customized databases, and organizing and publishing research results.

For more information about the NASA STI program, see the following:

- Access the NASA STI program home page at *http://www.sti.nasa.gov*

- E-mail your question via the Internet to help@sti.nasa.gov

- Fax your question to the NASA STI Help Desk at 443-757-5803

- Phone the NASA STI Help Desk at 443-757-5802

- Write to:
  NASA STI Help Desk
  NASA Center for AeroSpace Information
  7115 Standard Drive
  Hanover, MD 21076-1320

NASA/TM–2011-217145

A Data System for a Rapid Evaluation Class of Subscale Aerial Vehicle

Edward F. Hogge
Lockheed Martin, Hampton, Virginia

Cuong C. Quach and Sixto L. Vazquez
Langley Research Center, Hampton, Virginia

Boyd L. Hill
Vigyan Inc., Hampton, Virginia

National Aeronautics and
Space Administration

Langley Research Center
Hampton, Virginia 23681-2199

May 2011

Available from:

NASA Center for AeroSpace Information
7115 Standard Drive
Hanover, MD 21076-1320
443-757-5802

Abstract

A low cost, rapid evaluation, test aircraft is used to develop and test airframe damage diagnosis algorithms at Langley Research Center as part of NASA's Aviation Safety Program. The remotely operated subscale aircraft is instrumented with sensors to monitor structural response during flight. Data is collected for good and compromised airframe configurations to develop data driven models for diagnosing airframe state. This paper describes the data acquisition system (DAS) of the rapid evaluation test aircraft. A PC/104 form factor DAS was developed to allow use of Matlab®, Simulink® simulation code in Langley's existing subscale aircraft flight test infrastructure. The small scale of the test aircraft permitted laboratory testing of the actual flight article under controlled conditions. The low cost and modularity of the DAS permitted adaptation to various flight experiment requirements.

Nomenclature

α = angle of attack, deg.
β = angle of sideslip, deg.
δ_a = aileron deflection, deg.
δ_e = elevator deflection, deg.
δ_r = rudder deflection, deg.
Ψ = Euler yaw angle, deg.
Θ = Euler pitch angle, deg.
Φ = Euler roll angle, deg.
ADC = Analog to Digital Converter
AHRS = Attitude and Heading Reference Sensor
AirSTAR = Airborne Subscale Transport Aircraft Research
BIOS = Basic Input Output System
c.g. = Center of Gravity
COTS = Commercial off-the-shelf
CPU = Central Processing Unit
DAS = Data Acquisition System
DOS = Disk Operating System
EMC = Electromagnetic Compatibility
EMI = Electromagnetic Interference
FASER = Free-flying Aircraft for Subscale Experimental Research
GPS = Global Positioning System
IMU = Inertial Measurement Unit
INS = Inertial Navigation System
I/O = Input/output
ISA = Industry Standard Architecture (IBM PC bus standard)
PC-AT = IBM PC with "advanced technology" bus standard
PSD = Power Spectral Density
R/C = Remote Control
RAM = Random Access Memory
RPM = Revolutions per minute
UAS = Unmanned aerial system

Introduction

The use of a low-cost subscale unmanned aerial system (UAS) enables high risk research experiments to be flown under realistic conditions unavailable in a laboratory or computer simulation setting. The low cost and lower risk as compared to human piloted flight testing allow a wider range of flight experiments to be considered. The SIG Edge 540T subscale test aircraft is built from a kit by SIG Manufacturing Company, Inc. It is an inexpensive and spacious platform for the necessary sensors and computer processing electronics (Figure 1). The test aircraft is a 1:33% subscale version of the Zivko Aeronautics Inc. Edge 540 T tandem seat aerobatic aircraft.

This report describes the instrumentation used for the Edge 540T test aircraft research. The experiments flown using this platform include 1) development of an algorithm to

Figure 1: View of the Edge 540T R2 Test Aircraft (Photo Courtesy of Tom Vranas) [11]

diagnose damage to the wing spar structure using actual damage, 2) development of an algorithm and hardware to predict time to depletion of the propulsion batteries, 3) a software health experiment testing runtime techniques for monitoring avionics software.

A high-level language simulation environment was chosen for the airborne data acquisition system (DAS). The MathWorks® Matlab, Simulink, and Real-Time Workshop® real-time operating system provides a familiar development environment for mechanical, aeronautical, and electronics engineers. The low cost remotely piloted vehicle with a research computer compatible with the MathWorks tool chain built on earlier work demonstrated by the Langley Research Center Free-Flying Aircraft for Sub-scale Experimental Research (FASER) [1]. See Figure 2.

To the extent possible, the FASER architecture [2] was adopted so that available resources could be devoted to studying the airframe diagnosis and other experiments without having to go through a hardware and tool selection process redundantly. Existing I/O device drivers reduce the development effort, and standard data file formats enable easier collaboration across research organizations. Some file formats used include Matlab matfile (.mat) for engineering parameters and Microsoft Excel Workbook (.xls) for calibration and signal lists. The Airborne Subscale Transport Aircraft Research (AirSTAR) test bed project provided a Simulink software block diagram library of data acquisition software modules and aerodynamic calculation modules. These were used for the airborne DAS and as a starting point for a rudimentary simulation.

Laboratory motion experiments were done with a hardware-in-the loop version of this simulation to drive a motion base. An open source file configuration management process used in other AirSTAR experiments was used as well. Some changes were made to take advantage of the FASER experience, but on an airframe more suitable for

Figure 2: View of the FASER Ultra Stick 120 Test Aircraft [2]

structural testing. The limited size of the FASER Hangar 9 UltraStick 120 test aircraft fuselage [2], width 4.7 in., relative to the DAS flight stack, 3.5 in., made wiring changes difficult.

The larger Edge 540T R2 subscale test aircraft facilitated the integration of the electronics package and permitted flexibility in sensor wiring. The larger fuselage width, 12.5 in., and the larger payload capacity from the larger weight, 41 lbs., increased the number of feasible experiments. For comparison, the fuselage width of the FASER was 4.7 in. and the weight was 16.5 lbs. Spare payload capacity of the Edge accommodated multiple experimental payloads per flight. The use of a sizeable removable cockpit facilitated the alignment and software integration of the attitude and GPS sensors as the sensors could be treated as a self-contained subsystem. Accessibility was improved and compass alignment and other tests performed without the large airframe being involved. This configuration permitted work on the avionics, airframe, and power plant to proceed in parallel.

Other Edge UAS features included a COTS data system to measure selected vehicle parameters. A ground tracking camera, an on-board wing camera, and a research maneuver event marker were used to identify research maneuvers and check the logged attitude data.

Edge 540 Data Acquisition System

The on-board data acquisition system (DAS) for the Edge 540 Subscale UAS was designed to acquire and log engineering parameters during a 10-15 minute flight operation. The data system was also designed to operate with laboratory experiments of wing spar damage using a motion base to simulate flight maneuver loads. The DAS (Figure 3) consisted of a single board computer, boards to measure vehicle analog sensors, boards to condition signals, and a board to regulate power and a board for serial communications.

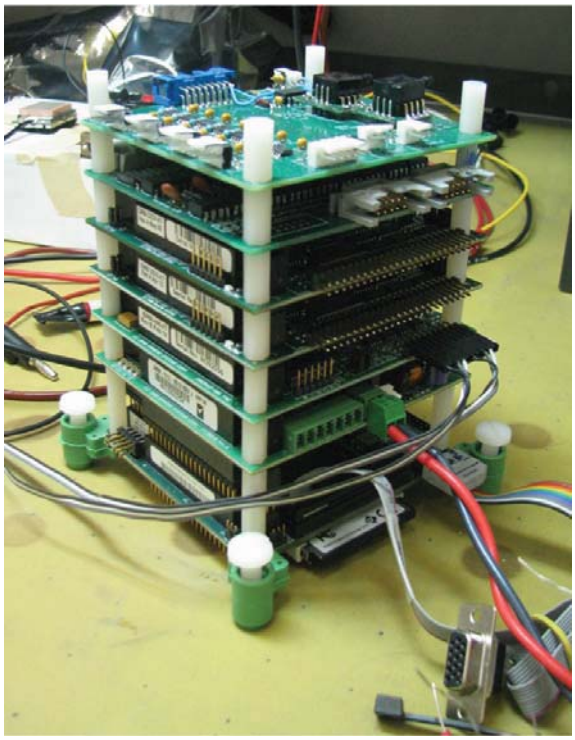

Figure 3: Edge 540 R2 DAS Flight Stack on the Bench

The DAS computer is an Ampro Core Module 620 Single Board Computer. It has an AMD Geode™ LX 800 processor and complies with the PC/104 form factor standard (Figure 4). The single board computer has the PC-AT architecture to execute the code generated from a Simulink model using the xPC Target® real-time operating system [3]. This environment corresponds to a similar laboratory hardware in-the-loop Matlab/Simulink simulation environment. This is a platform familiar to developers and compatible with the AirSTAR software architecture [4]. It allows use of high-level block diagram programming tools and also fits within the weight and vibration constraints of the test aircraft environment.

The CPU speed is moderate by today's desktop machine standards as indicated by the comparison in Figure 5. However, it uses low power and does not require a cooling fan. It has 512 MB of plug-in RAM. A compact flash disk drive, 8 GB, stores the logged data. File size is constrained by the 32-bit addressing of the file conversion program provided. This permits a 25-minute recording of logged channels at a 500Hz sampling rate.

The DAS block diagram (Figure 6) shows various communications and measurement interfaces for components listed in Table 1. Two 32-channel analog input and output (I/O) modules, 4-channels of serial communication RS-232 and an Ethernet I/O module are present. An attitude and heading reference sensor (AHRS), a Global Position System (GPS) sensor and an optional user payload are attached through serial RS-232 ports. Voltage level shifters for the RS-232 channels allow use of "hot swapping" of the

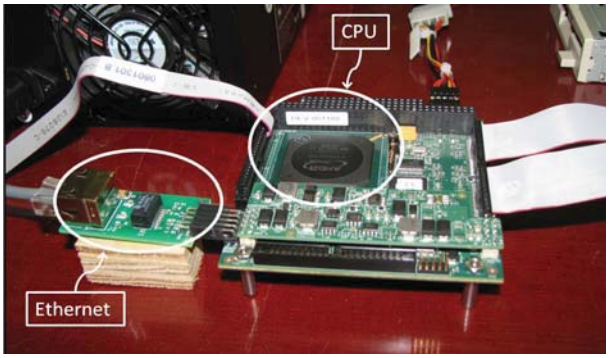

Figure 4: AMD Geode 500 MHz CPU and Ethernet Daughter Board

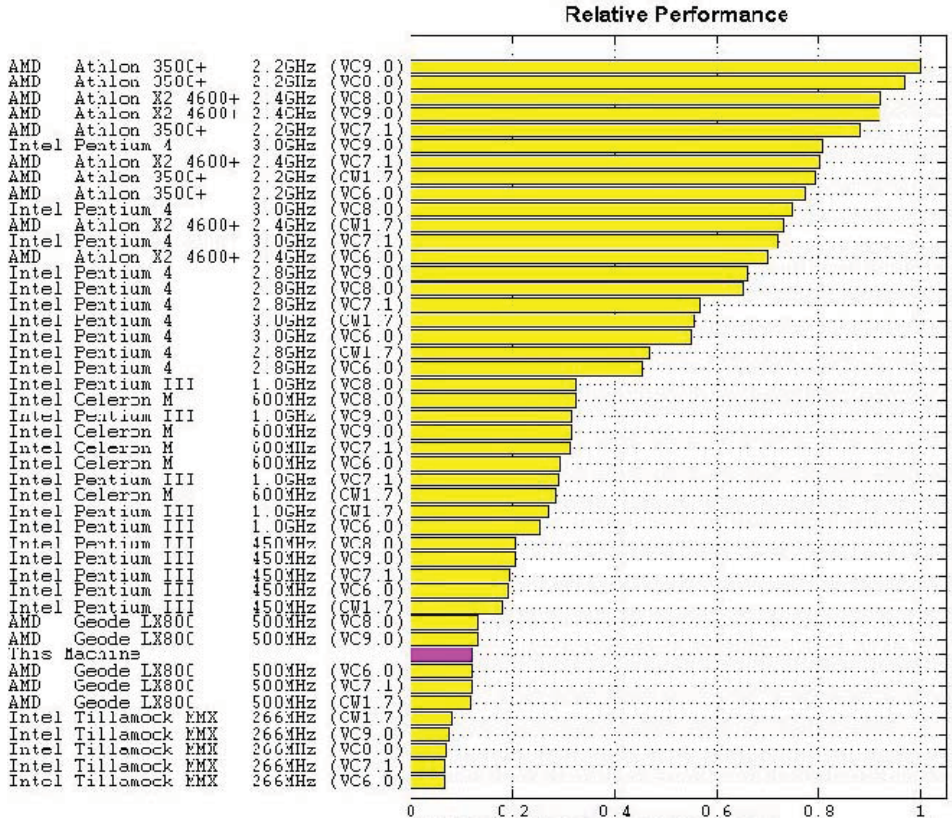

Figure 5: AMD Geode LX800 CPU on DAS Main Board Comparison with Typical Desktop PC Computer Processors [10]

canopy serial lines according to the RS-232 standard. Figure 6 depicts the data bus and major system cable connections. The CPU board is at the bottom of the stack and provides the best time source for synchronizing parameter measurements. The 500 Hz sampled analog boards (blocks analog I/O 1 and 2) have the tightest time synchronization. The AHRS and GPS ASCII code stream are logged asynchronously at 20 Hz and 1 Hz respectively.

A user payload can be optionally logged at 10 Hz. A 2 Hz sine wave analog signal is produced by analog output and serves as a simple time reference for other on-board data systems. It also serves as a system activity monitor when added to the downlink telemetry stream and provides situational awareness of DAS system health during flight operations.

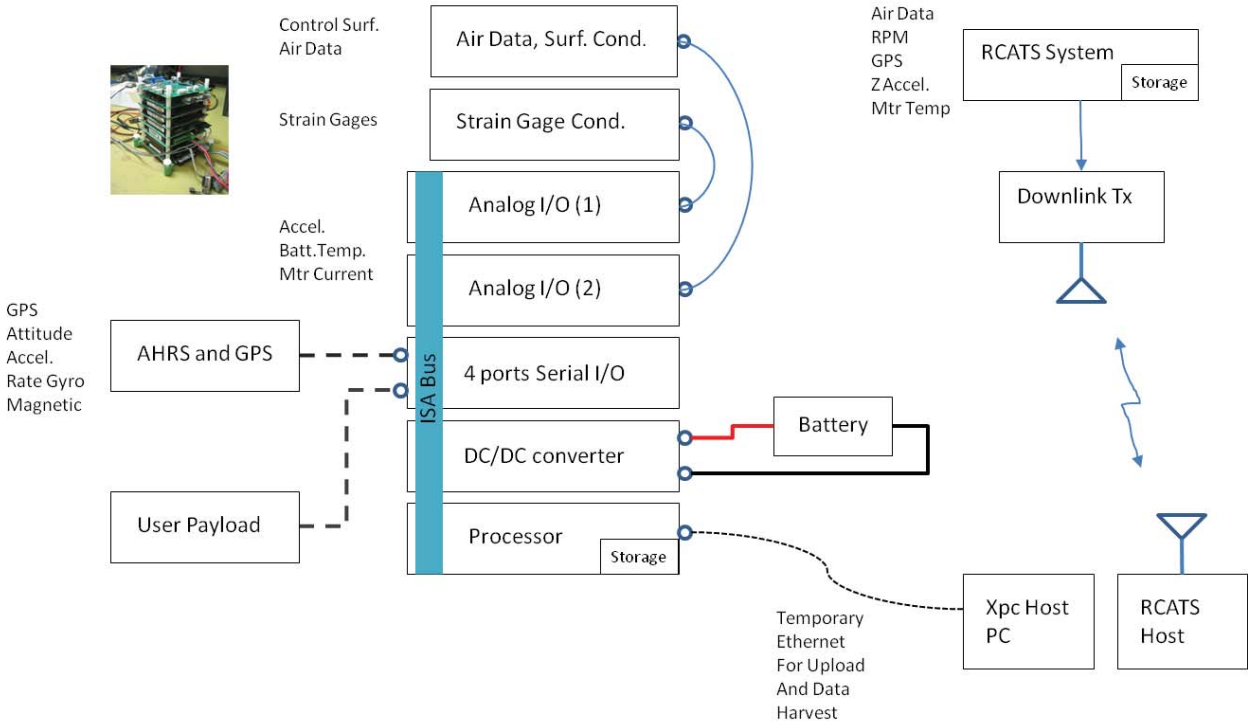

Figure 6: Block Diagram of the Edge 540T R2 DAS

Table 1: Primary DAS Components

Component	Manufacturer	Model or Part Number	Specifications
Computer	AMPRO Computers Inc.	CoreModule 620 AMD Geode	PC/AT, 500MHz CPU, 512 MB Memory, 2 Serial, 2-USB ports, 10/100 Base T and TX Ethernet
Compact Flash	Kingston Technology	CF/8GB	IDE 3.3V, 8GB
Analog I/O	Diamond Systems	DMM-32DX-AT	A/D: 32 Ch. SE, 16 bit, 250K sample rate, auto calibration D/A: 4 Ch. 12 bit
DC/DC Power Supply	Diamond Systems	JMM-512-V512	50W, +5V, 10A; +12V, 2A -5V, -12V outputs
Serial I/O	Diamond Systems	Emerald-MM	4-Channel RS-232
Serial I/O level shifter	Acroname, Inc.	R115-INT-BRD-1	+-12V conversion to TTL
Telemetry transmitter	RCAT Systems	RCATS™-UAV	900MHz Telemetry 10 Hz sampling
Attitude Heading Reference System (AHRS)	VectorNav	VN-100	3-axis accel./gyro/magnetometer INS solution Accelerometers: +-6g, non-linearity 0.5% of FS Gyros: +-500 deg/sec, non-linearity 1% of FS
GPS antenna/sensor	USGlobalSat, Inc.	EM-406A	1 Hz NMEA output command
Air Data Vanes	RCAT Systems	Custom built	+-1 deg accuracy, 0.75 deg resolution, carbon fiber
Barometric Static Pressure	Freescale Semiconductor, Inc.	MPXAZ6115AP	45.9 mV/kPa, +-1.5% FS
Barometric Differential Pressure	Freescale Semiconductor, Inc.	MPXV7002DP	1000 mV/kPa +-2.5% FS
Wing Accelerometers	Analog Devices	EVAL-ADXL335Z	Accelerometers: +-3.6g, non-linearity .3% of FS
Wing Strain Gages	Measurements Group, Inc.	CEA-060187UW-350	Constantan, Gage Factor 2.085 +-0.2%
Wing Spar Strain Gages	Measurements Group, Inc.	WK-13-125AD-350	K-alloy, Gage Factor 2.09 +- 1.0%

Figure 7 is the Simulink diagram for the normal configuration of the DAS. The two blocks in the upper left are the analog input card device drivers. The lower half of the diagram show the blocks associated with the RS-232 serial I/O streams. Two VectorNav VN-100 attitude devices, a GPS device, and an optional user payload serial device emit a serial character stream which is logged to the PC/104 single board computer flash memory. This diagram is converted to C-code by the Real-Time Workshop code generator and

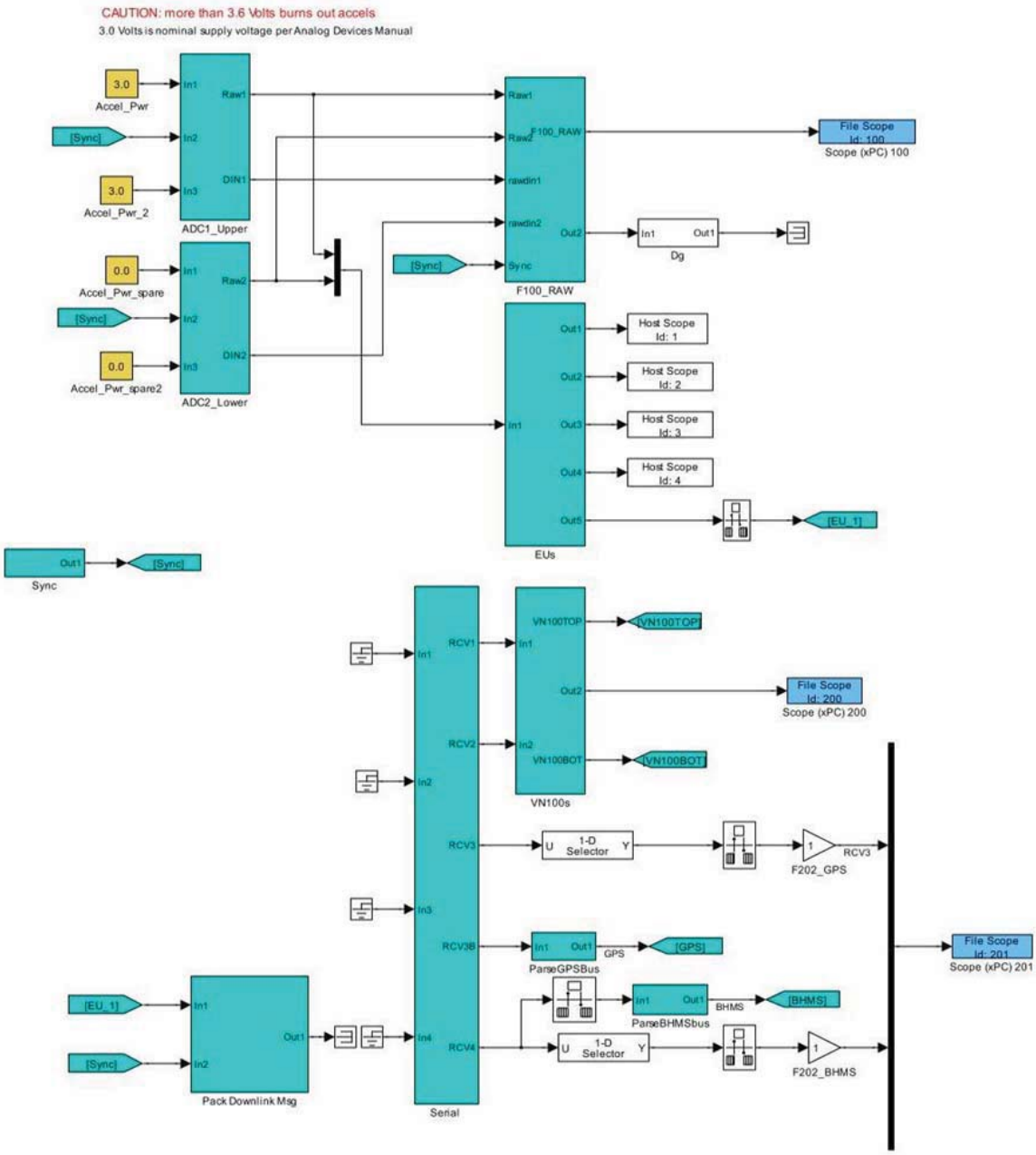

Figure 7: Simulink Diagram of the DAS, Normal Software Configuration

downloaded to the real-time operating system xPC Target.

RCATS telemetry system

A COTS data system, RCATS, Figure 8, is present to provide altitude and airspeed information to the remote pilot. It has a low speed transmitter to downlink selected parameters at 10 Hz during flight. It functions during the development of the Research DAS to give a reliable air speed and altitude ground read out to assist the pilot. Once confidence is gained in the Research DAS it can be removed. The Research DAS and the RCATS each logged engineering parameters using on-board compact flash memory.

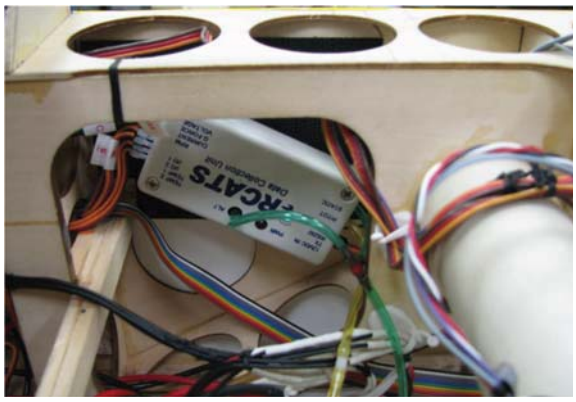

Figure 8: RCATS System for Altitude and Airspeed for the Remote Control Pilot

Table 2: RCATS Sensors and Sampling Rate

Sensors	**Locations**	**Analog Signals**	**Rate**
Structure Characterization			
CG acceleration	1 position (z)	1	10 Hz
Aerodynamic Characterization			
Airspeed	Pitot RCATS Total and Static port	1	10 Hz
Altitude	RCATS Pitot Static port	1	10 Hz
Propeller RPM	Spinner RCATS™ (Hall effect sensor)	1	10 Hz
Flight Management			
Position	GPS RCATS (Lat, Lon, Alt)	3	1 Hz
Position	GPS USGlobalSat	3	1 Hz
Motor temperature	motor housing	1	10 Hz

Table 3: Research DAS Sensors and Sampling Rate

Sensors	**Locations**	**Analog Signals**	**Rate**
Structure Characterization			
Strain	9 positions span wise	9	500 Hz
Wing acceleration	6 positions (x, y, z)	18	500 Hz
CG acceleration	2 positions (x, y, z)	6	500 Hz
Motor Mount acceleration	1 position (x, y, z)	3	500 Hz
Event marker	N. A.	1	500 Hz
Aerodynamic Characterization			
Attitude Heading Reference Sensor	1 position (yaw, pitch, roll)	3	20 Hz
Attitude Heading Reference Sensor	1 position attitude(quaternion) magnetic vector acceleration vector body rotation rates	4 3 3 3	20 Hz
Airspeed	Pitot Total and Static port	1	500 Hz
Altitude	Pitot Static port	1	500 Hz
Ambient Temperature	1 position	1	500 Hz
Propeller RPM	Spinner (Hall effect sensor)	1	500 Hz
Ailerons	2 positions	2	500 Hz
Elevators	2 positions	2	500 Hz
Flaps	2 positions	2	500 Hz
Rudder	1 position	1	500 Hz
Flight Management			
Motor Current	motor speed controller	2	500 Hz
Motor battery temperature	motor batteries	4	500 Hz
Motor battery currents	motor batteries	4	500 Hz
Motor battery voltages	motor batteries	4	500 Hz

The logged measurements for the DAS are harvested by Ethernet download at the end of the flight while the logged measurements for the RCATS are harvested by the removal of flash media. The parameters logged are listed in Table 2 and Table 3.

Signals Logged by the DAS

Table 3 is a list of location and sampling rates for the research data sensors. Structure characterization instrumentation consists of wing structure strain gages and wing accelerometers.

Aerodynamic model characterization instrumentation consists of total and static probe barometric sensors for altitude and airspeed. The probe is also fitted with vanes to measure angle-of-attack (α) and angle-of-sideslip (β). The propeller revolution speed sensor gives a thrust measurement, an inertial navigation position and orientation sensor, and a 3-axis roll rate sensor give kinematic motion parameters yaw (Ψ), pitch (Θ), and roll (Φ). The aileron (δ_a), elevator (δ_e), rudder (δ_r), and flap deflection signals are necessary for control input configuration for the aerodynamic model identification.

Other sensors record parameters related to vehicle health such as battery voltage, battery current, battery temperature, and propulsion motor current. The DAS logs these sensors, and selected ones are plotted for a typical flight in Figure 9. The static pressure, which is inversely related to altitude, defines the extent of the flight from takeoff to landing. It is seen in the fourth strip chart of Figure 9. The first strip chart depicts the current to one of the propulsion motors and reaches a maximum of 100 Amperes during the takeoff climb to altitude. The event marker trace is high during two straight track cruise maneuvers to take data for a structural failure diagnosis experiment completed at 360 seconds.

The two periods of zero current that follow are two stall maneuvers with two flap settings as shown in the parallel third strip chart, green trace. Even though the throttle was completely off and no current was commanded to the propulsion motors, the propeller revolutions per minute (RPM) did not go to zero because the motors are programmed to free wheel when off, allowing the propeller to be driven by the apparent wind produced by the forward motion. After the landing at approximately 520 seconds, the activity in the strip charts between 620 to 680 seconds is due to a taxi along the runway back to the flight line.

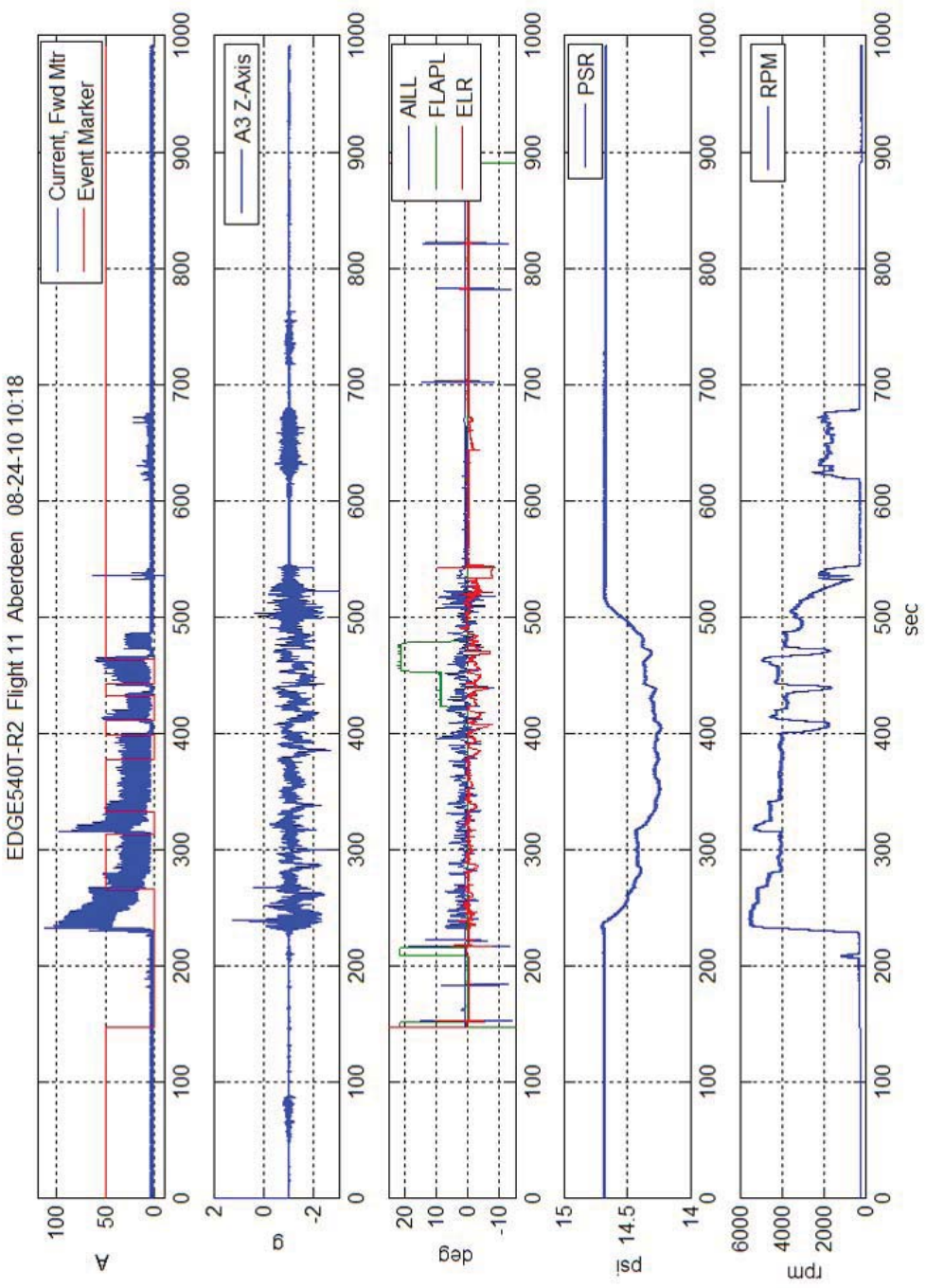

Figure 9: Selected Parameters from a Typical Flight

Attitude and GPS Sensor

A range of INS options are available for this size vehicle. Since the structural damage diagnosis research did not have a stringent accuracy requirement on the estimate of attitude and rotation rates, a lower cost system was selected. The lower cost system did not integrate the GPS measurements with the attitude inertial sensors but rather relies on the local magnetic and acceleration measurements to obtain an attitude solution.

A VectorNav VN-100 attitude heading reference sensor (AHRS) was used. This was located near an USGlobalSat GPS sensor under the canopy, Figure 10. The attitude sensor's default state worked acceptably in pitch and roll, but yaw exhibited spurious mirror image rotation reversals and nonlinearity dependent upon compass quadrant heading. This effect was in the recorded data and is not easily corrected. The factory default for the assumed orientation of the Earth magnetic vector was that of the Western U.S. The reference Earth magnetic vector was corrected to the orientation of the Eastern U.S.

To reduce vibration effects, the accelerometer's contribution was deemphasized and the magnetometer's and rate gyros' contributions emphasized in the Kalman INS solution. This solved the problem of rotation reversals during taxi and ground operations. However, the problem persisted during flight and is believed to be propeller vibration-related. A possible mitigation strategy being considered is to soft-mount the sensor.

A nonlinearity problem in heading (yaw) was addressed by sampling of all orientations to make corrections of hard and soft iron effects (Figure 11). A non-ferrous level table

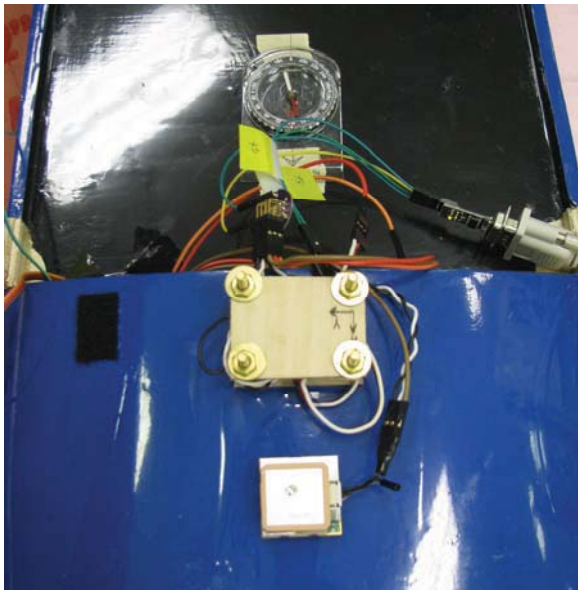

Figure 10: VN-100 Attitude Sensor and USGlobalSat GPS Sensor Shown with Compass used During Alignment.

oriented North/South was used to establish attitude correction factors with the avionics operating. It had been anticipated that the strong magnets in the electric propulsion motors would bias the Earth reference magnetic field, but this effect was negligible at the installation location of 26 inches

Figure 11: Laboratory Use of Non-magnetic Level Table for Hard/Soft Iron Compensation of AHRS Magnetic Reference Vector

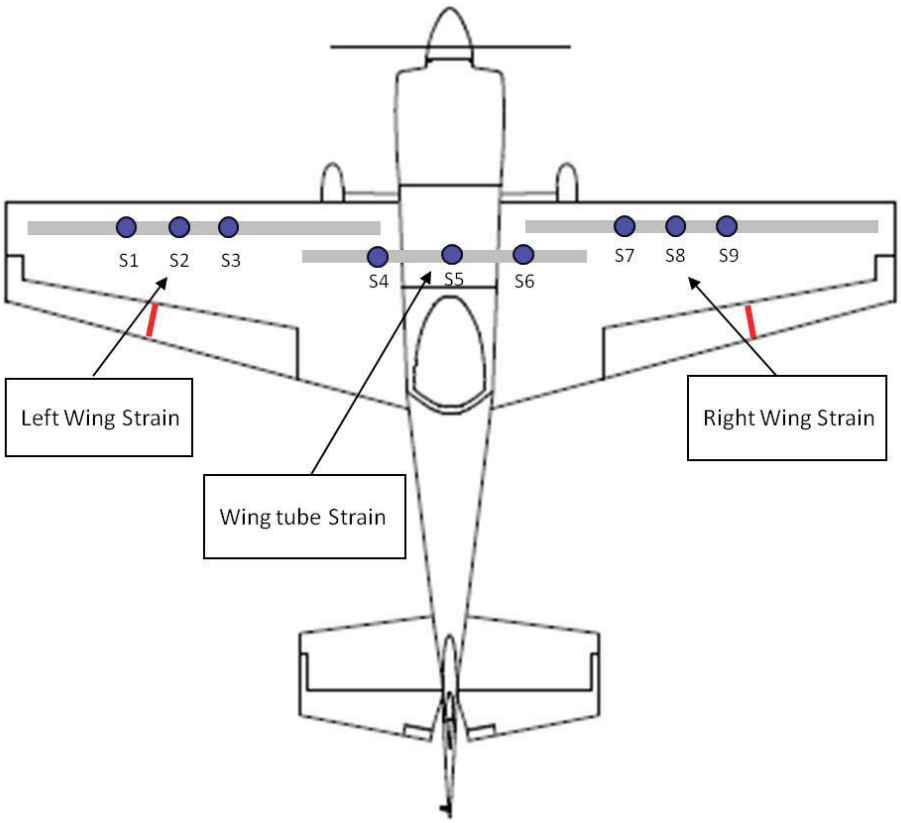

Figure 12: Strain Gage Locations

between the motor and the attitude sensor.

EMC Testing

As a matter of precaution, EMC testing is performed on various aspects of the instrumentation and control electronics [5], [6]. Procedures call for a radio range test to be performed before each flight deployment. This is described in [5]. An emissions study was performed on the installed instrumentation in a reverberation chamber. This is described in [6].

This section describes an early evaluation of potential interference on strain gauge data channels from sources associated with the Edge airplane. Of particular concern are the transmitters for the remote control (R/C), the RCATS, and the XBEE™ alternative downlink. (The XBEE transmitter was used

to configure the attitude inertial sensor before flight and turned off during flight because of this interference. It was removed during later flights because the attitude system could be configured in the laboratory more effectively.)

For this evaluation the DAS was started in record mode. Then the three systems were started up and shut down and the control surfaces moved using the servos. Figure 14 plots the EMI effect on the strain gauge S4 located in left outboard position of the wing tube as diagrammed in Figure 12 and Figure 13.

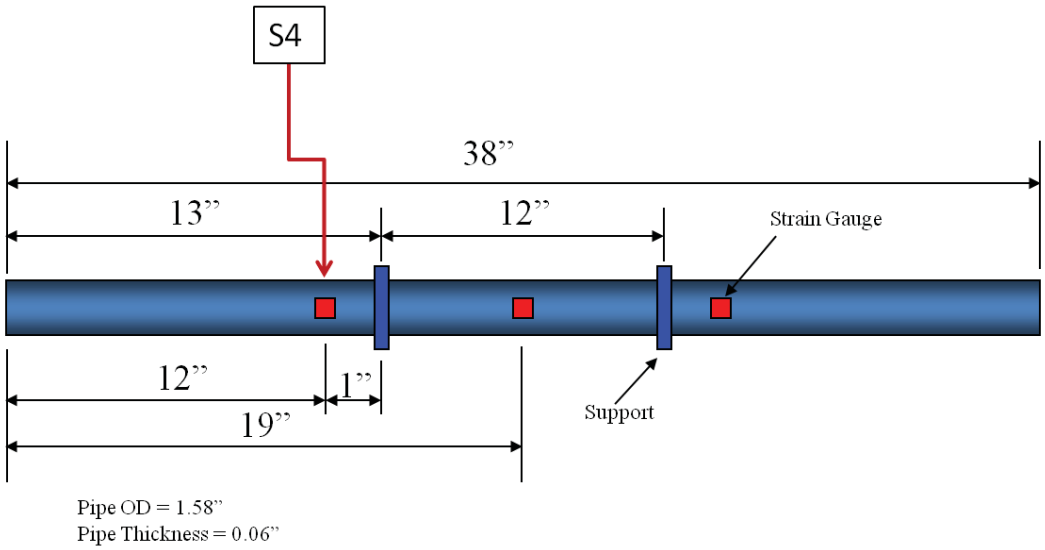

Figure 13: Wing Spar Detail of Strain Gage Locations

The Edge is piloted using a COTS JR-12X™ control radio. It is a robust remote control (R/C) system which reduces the probability of self-interference by executing a frequency selection process during the transmitter and receiver start up as described in [5]. The sophistication of the JR-12X enables it to avoid congested frequencies in the 2.4GHz band but appears to impart some measurable signals on the S4 during the selection process. As seen in Figure 14, the selection process initially created spikes on the S4 strain signal. The initial spikes became quiet once the negotiation was complete.

A test motion of a control surface by a servo caused loading of strain gage S4 through excitation of a natural resonant vibration mode that moved the wing. This is the spike following the “command servo motion” annotation.

Selection of a frequency away from self-interference sources such as the PC104 CPU clock (500 MHz) made the control system more robust than the technology available during FASER development [2]. Diversity of receiver locations also may have helped. A proof test was done on the ground as a build-up to flight and as a part of the laboratory verification of control functionality before flight. Two telemetry data links were also tested for self-interference. The XBEE telemetry data link transmitter imparted enough power to the twisted pair strain gage wiring that the low-voltage strain signals were overwhelmed. Unshielded twisted-pair strain gage wiring was used to simplify cable fabrication and reduce weight.

Better EMI rejection may result from shielding and enclosure of the data logging computer and power system, at the cost of weight, space, and flight duration, so was not implemented for these flights. This is discussed in [6].

The RCATS telemetry transmitter exhibited a much smaller effect on the low-voltage strain signals, below a significant fraction of the signal level. It was used in flight to relay altitude and airspeed. The annotations in Figure 14 describe when each subsystem was turned on and off during a self-interference test.

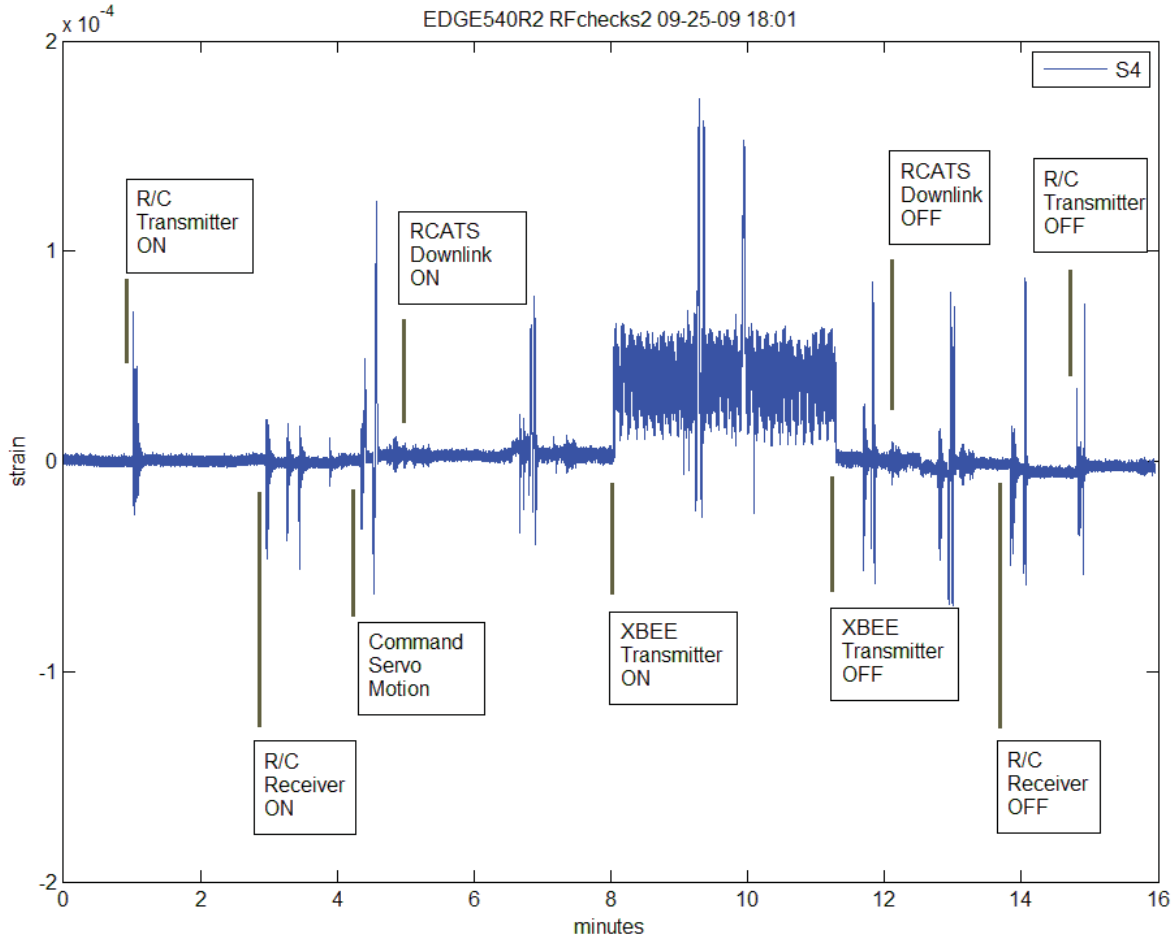

Figure 14: Self-Interference Effects on Left Wing Spar Strain Gage Signal

Live Propeller Vibration testing

A live propeller was operated with the test aircraft secured with a steel cable to the wall of the NASA Langley Research Center High Intensity Research Facility Reverberation Chamber. The aircraft was powered up in flying configuration with battery power to the motor and data logging electronics. The aircraft was controlled through a rebroadcast of a control signal from the control room to the test cell. The research test pilot commanded the motor to maintain 4000 RPM (67 Hz) and the aircraft sensors were logged by the Edge540 DAS. The accelerometers were located as shown in Figure 15. One run was performed with the acceleration sensor powered off to record any EMI effects on the passive channels. Other runs were done with the acceleration sensors powered on as during normal operations. This way, the measurement effects due to vibration could be separated from those due to EMI.

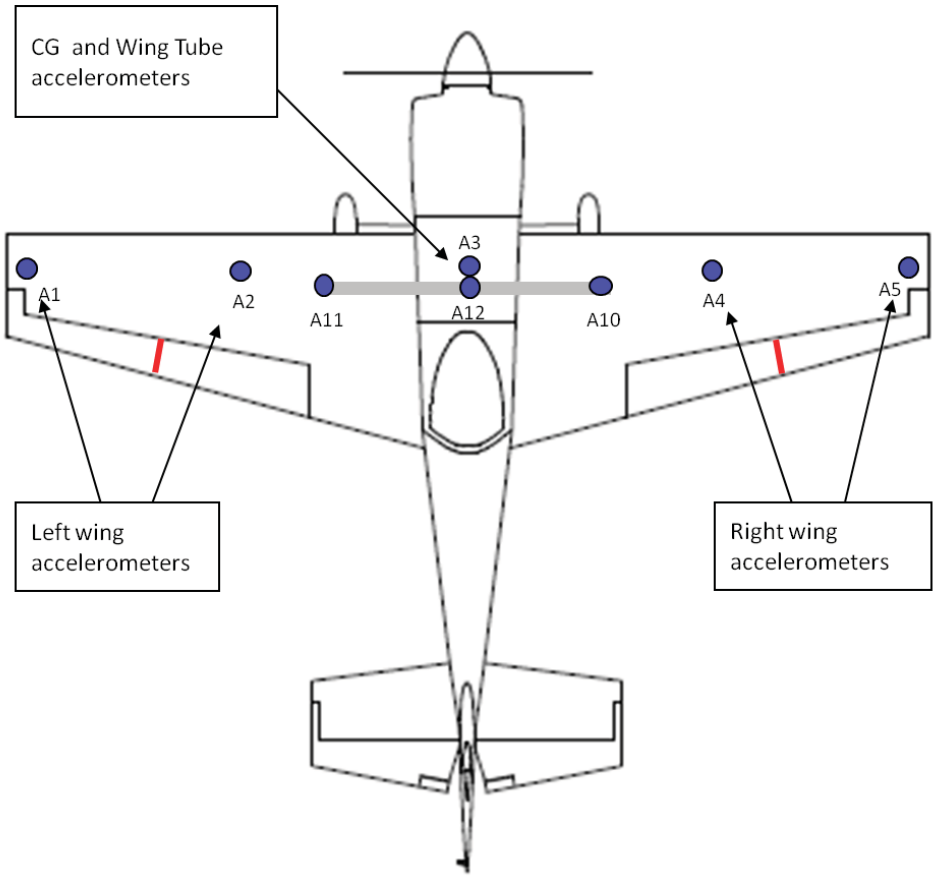

Figure 15: Accelerometer Locations

Figure 16 shows a combined plot of the power spectral density (PSD) of the vertical axis (Z) component of the accelerometer at the nominal center of gravity (c.g.). The blue trace is with the accelerometer preamplifier powered on. The red trace is with the accelerometer preamplifier powered off. A low-pass 50-Hz filter was present at the sensor to prevent aliasing. This test was performed at a high sampling rate (2200 Hz) compared with a 200 - 500 Hz nominal sampling rate for research flights. A Hamming window [7] using Welch's method was used to process the data to generate the PSD [8]. The spikes on the blue trace were due to the propeller frequency and its harmonics. No evidence of the propeller spikes can be seen on the red trace. The periodic ripple is an artifact of the windowing method. This indicates that there was no significant EMI problem with the acceleration data path because the signal's envelop decays below 40dB in the region of interest.

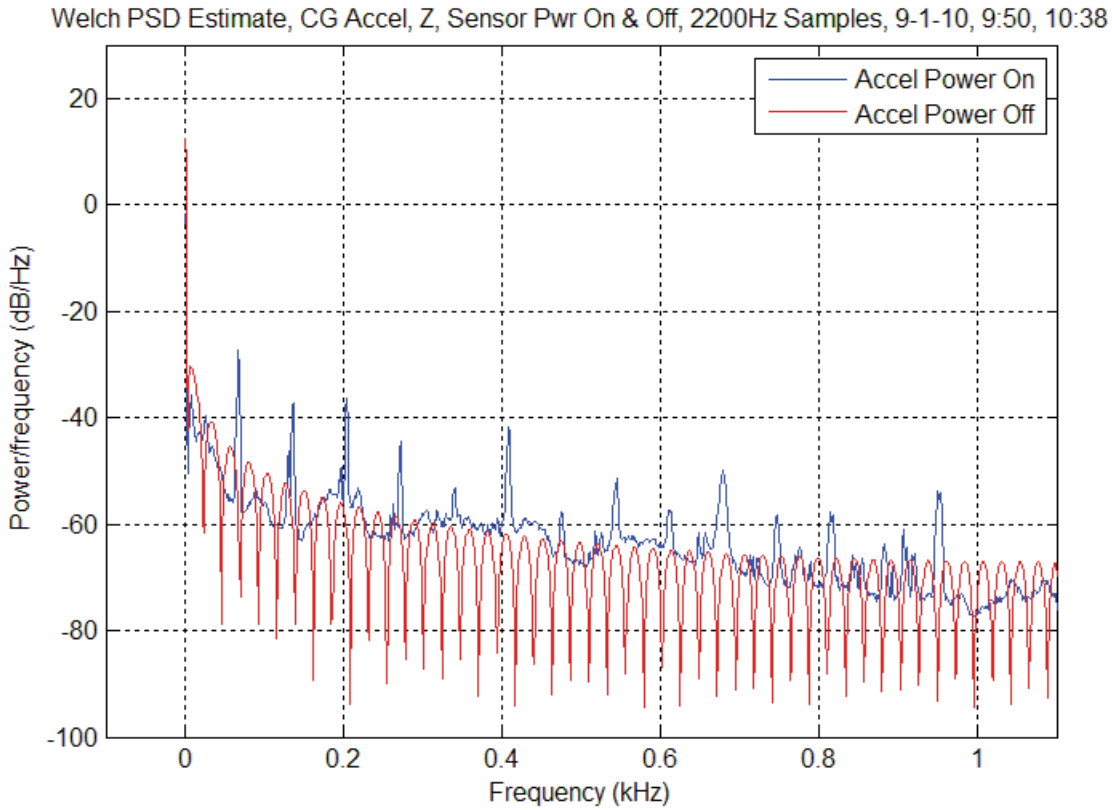

Figure 16: Power Spectrum of the C.G. Accelerometer with the Sensor Power On and Off

There was an additional concern that the first and second harmonics of the propeller frequency were aliasing into the data as a lower frequency when the DAS was sampling at 200 Hz. Based on this test the sampling frequency was increased to 500 Hz to reduce any aliasing effects during the subsequent damage detection flights.

Another view of the vibration test is given by a time domain plot of the three tube (wing spar) strain gages, followed by various accelerometers, Figure 17. The accelerometer plot starts with the one at the test aircraft c.g. followed by the one at the tube center. The others are progressively further along the left wing. This is a one-tenth second snapshot to give the flavor of the synchronized response to the propeller vibration forcing input. Since this was a simpler dynamical configuration compared with free flight it may provide insight to help analyze the flight data. The reaction force of the aircraft wheels against the support surface may cause stronger acceleration readings than the case of free-flight.

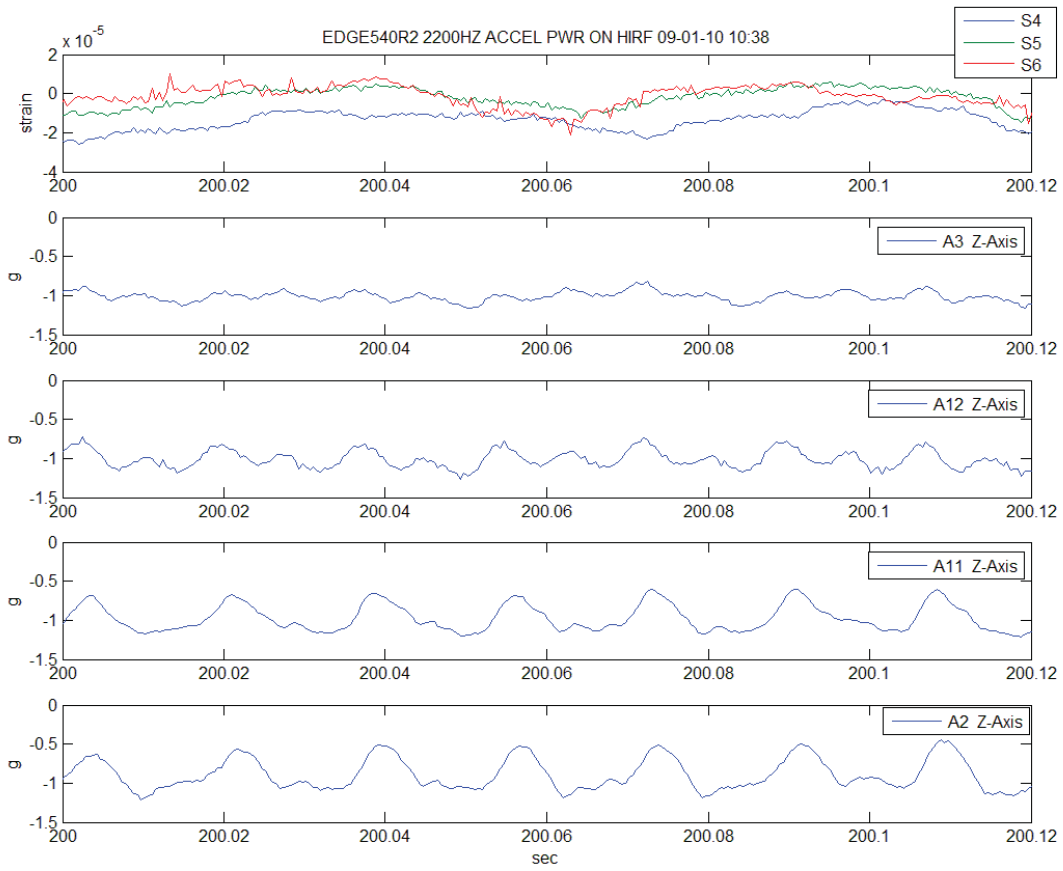

Figure 17: Vibration Time History at Stations from the Aircraft c.g. to the Middle of the Left Wing

Issues

Some integration problems encountered were propeller vibration-related. The anti-aliasing filtering of the acceleration measurements did not suppress the propeller frequency adequately for the initial 200 Hz sampling rate. This was revealed by ground facility EMI testing and a flight flown with selected DAS channels sampled at a much higher rate to identify the actual noise spectra. The sampling rate was increased to 500 Hz and the number of data channels recorded reduced to stay within processor limitations. An attempt to employ a low-cost attitude sensor was made, but the yaw axis measurement was compromised by similar vibration effects.

Conclusion

The use of commercial off the shelf hardware with a large subscale model facilitated rapid development. The adaptable software environment facilitates changes and adaptation of payload experiments. Testing of high risk experimental algorithms and avionics packages is possible with minimum project risk due to low cost. Vibration and EMI problems give experimenters the realism necessary to see their prototype devices and ideas behave in a flight environment with minimal risk as compared with a full scale flight. Vibration and EMI from telemetry transmitters present challenges for data quality, but AirSTAR standard control radio verification procedures assure flight safety.

Appendix

Sensor Calibration, Acceleration

The accelerometer channels were calibrated through use of the data system and a level table. The ADXL335 3-axis accelerometer evaluation board was attached to a holder that allowed it to be placed on the table and oriented parallel and anti-parallel to the local gravitational acceleration vector according to each of the three axes. The resulting measurements were fitted to a linear equation through use of the Matlab function "polyfit". The calibration covered 1/3 of the ±3g full scale range of the sensor. This was accepted as part of the low-cost philosophy. A plot of the acceleration as a function of the sensor output voltage for a typical sensor is given in Figure 18. Table 4 summarizes the linear equation gain and bias factors for the other accelerometers.

Table 4: Accelerometer Calibration Factors

Sensor		Gain	Bias
A1	X-axis	-3.33	4.76
A1	Y-axis	-3.34	4.92
A1	Z-axis	-3.35	5.08
A2	X-axis	-3.38	5.05
A2	Y-axis	-3.33	5.01
A2	Z-axis	-3.56	5.48
A3	X-axis	-3.38	5.00
A3	Y-axis	-3.37	5.05
A3	Z-axis	-3.38	5.08
A4	X-axis	-3.34	4.99
A4	Y-axis	-3.37	5.01
A4	Z-axis	-3.34	5.00
A5	X-axis	-3.36	5.03
A5	Y-axis	-3.36	4.98
A5	Z-axis	-3.36	5.03
A10	X-axis	-3.29	4.91
A10	Y-axis	-3.23	4.87
A10	Z-axis	-3.41	5.13
A11	X-axis	-3.37	4.97
A11	Y-axis	-3.33	4.99
A11	Z-axis	-3.38	5.11
A12	X-axis	-3.37	4.98
A12	Y-axis	-3.32	5.03
A12	Z-axis	-3.37	4.97

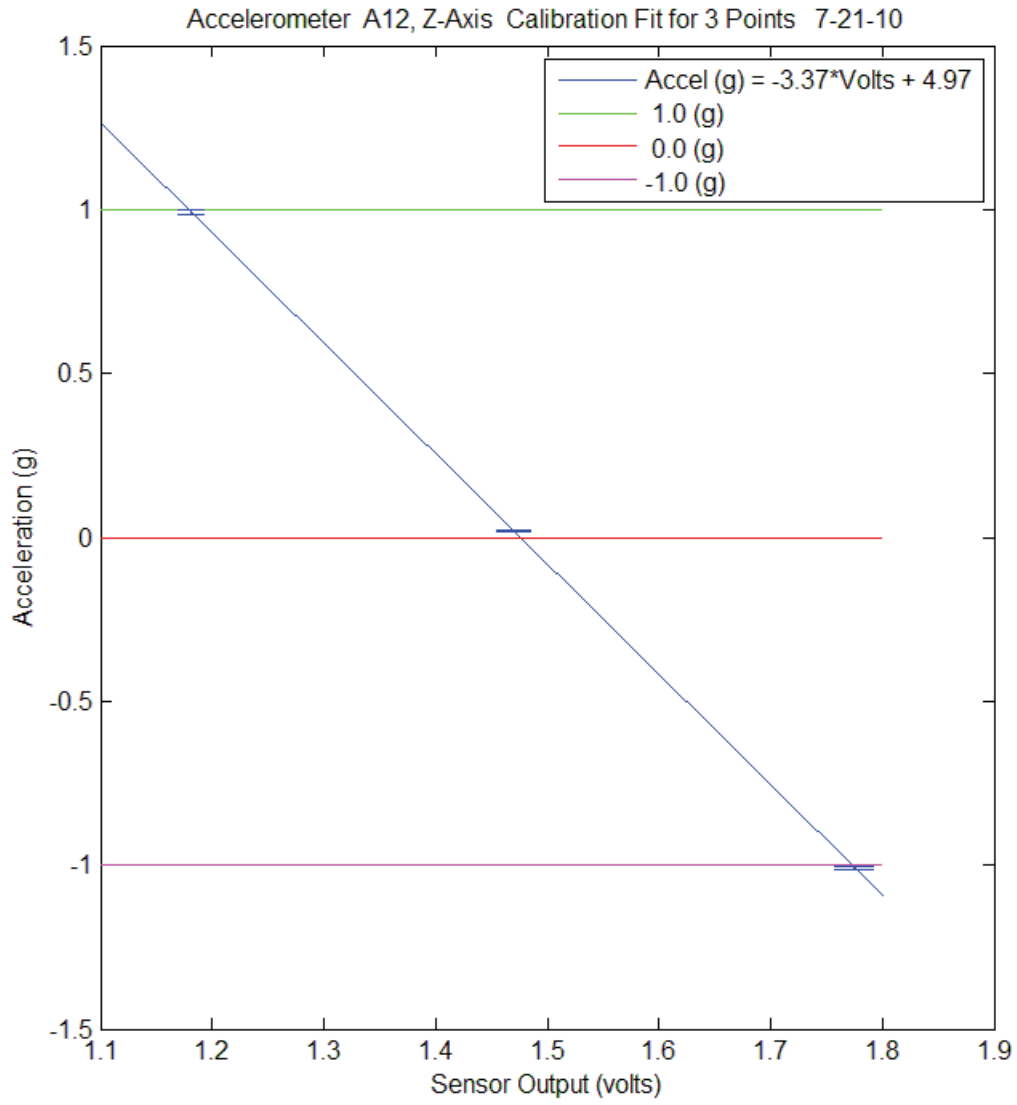

Figure 18: A 3-point Calibration Profile for a Typical Acceleration Sensor with Standard Error Bars and Measured Calibration Scattered Points.

Sensor Calibration, Control Surface Deflection

The control servos were modified by the attachment of pick-off leads on the potentiometer that is attached to the rotating actuator shaft. The DAS was operated as the surface was moved to zero degrees, the trailing edge up (TEU) deflection limit, and the trailing edge down (TED) deflection limit. The actual angle was measured using an alignment device [5]. The measurements were fitted to a linear equation similar to that of the accelerometers. A plot is given in Figure 19. Table 5 lists the linear equation fit gain and bias factors for the other control surfaces.

Table 5: Control Surface Potentiometer Calibration Factors

Sensor	Gain	Bias
AILL	7.93	-44.33
FLAPL	8.68	-47.39
ELR	-10.87	61.47
ELL	10.59	-55.87
FLAPR	-8.03	42.93
AILR	-7.62	41.83
RUD	-16.44	85.73

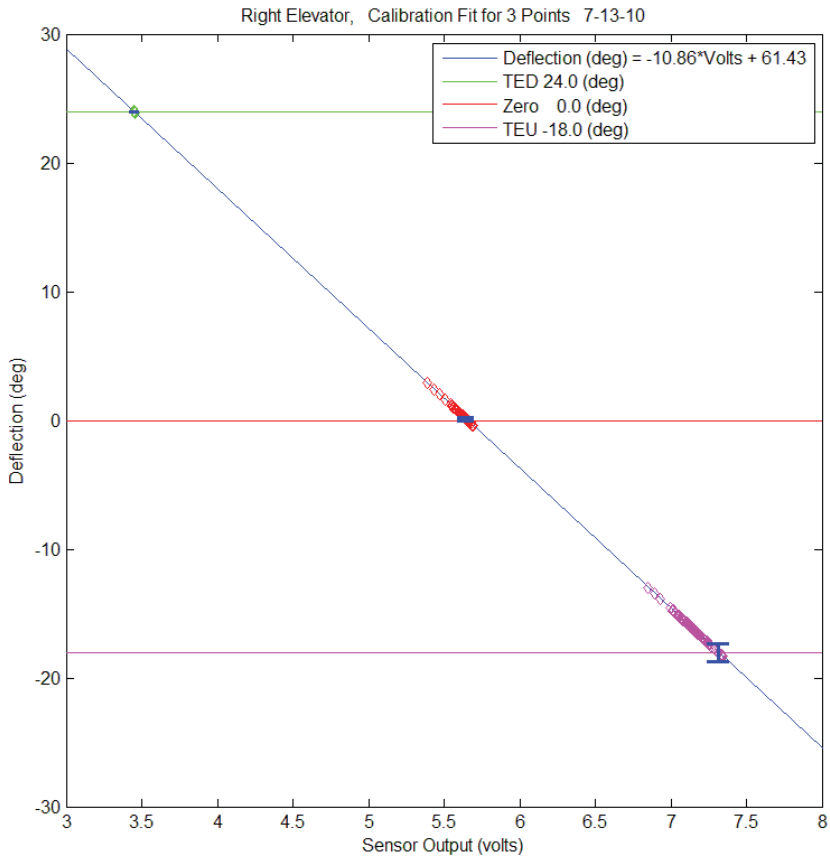

Figure 19: A 3-point Calibration Profile for a Typical Control Surface with Standard Error Bars and Measured Calibration Scattered

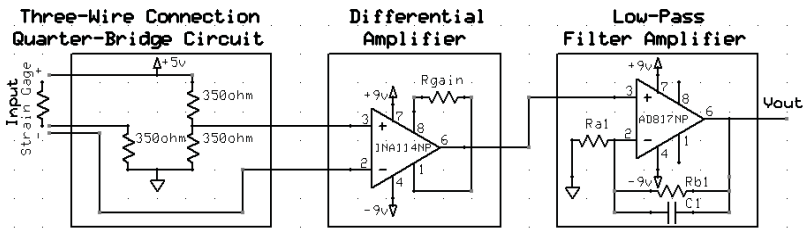

Figure 20: Signal conditioning circuit for each strain gauge position.

Sensor Calibration, Strain Gage

Nine strain gages are installed on the Edge to measure strain on the load path at various points as illustrated in Figure 12. Three gages are bonded to the spar cap on the top surface of each wing. The remaining three gages are installed on the aluminum load carry-thru tube on the interior surface. All strain gages are quarter-bridge foils, each wired to a signal conditioning circuit shown in Figure 20. The output voltages of these circuits are connected to the analog input channels on the DAS. A simple calibration technique was devised to obtain a voltage to strain conversion for the strain gage channels. For this, potentiometers were connected to the signal conditioning circuits in place of the strain gages. A series of DAS voltage measurements were recorded for potentiometer values ranging from 348 Ω to 352 Ω. The strains for the associated resistances are computed from the gage factor equation. [9]

$$GF = \frac{(R - R_G)}{\varepsilon \cdot R_G}$$

Solving for Strain:

$$\varepsilon = \frac{(R - R_G)}{GF \cdot R_G}$$

where: R_G is the 350 Ω nominal gauge resistance
R is the actual gauge resistance under test conditions
GF is the published gauge factor
ε is the strain

The calibration data (Table 6 and Table 7) includes the resistance values and the calculated strain and the voltages measured at the DAS. A second order polynomial fit is applied to the data in Table 6 and Table 7 to obtain a voltage to strain curve for the entire range. The results are given in Figure 21 for the DAS used in the aircraft. The polynomial fit coefficients are then used as conversion factors for converting voltage to strain for the strain channels on the DAS.

Table 6: Calibration measurements for wing strain gages

Resistance (Ω)	Ch1 (V)	Ch2 (V)	Ch3 (V)	Ch7 (V)	Ch8 (V)	Ch9 (V)	με
348.0	-4.1800	-0.0691	-3.2648	-7.6344	-2.0230	-5.3287	-2740
348.5	-3.4906	0.9324	-2.1632	-6.9145	-1.0283	-4.2249	-2055
349.0	-2.1410	2.1332	-1.2493	-5.6010	0.1397	-3.3397	-1370
349.5	-1.0557	3.1536	-0.0624	-4.5462	1.2217	-2.1403	-685
350.0	0.1262	4.2340	1.1513	-3.3638	2.2632	-0.9219	0
350.5	1.2771	5.0424	1.9840	-2.2387	3.1017	-0.0857	685
351.0	2.2975	6.4240	3.0939	-1.2000	4.4518	0.9627	1370
351.5	3.3824	7.5129	4.1772	-0.1311	5.5234	2.0942	2055
352.0	4.1265	8.4926	5.3469	0.6057	6.5468	3.3013	2740

Table 7: Calibration measurements for tube strain gages

Resistance (Ω)	Ch4 (V)	Ch5 (V)	Ch6 (V)	με
348.0	-4.5557	-0.3043	0.3132	-2734
348.5	-3.8375	0.6926	1.4211	-2051
349.0	-2.4150	1.8746	2.2990	-1367
349.5	-1.3779	2.9468	3.4887	-684
350.0	-0.2147	4.0073	4.7078	0
350.5	0.9449	4.8427	5.5418	684
351.0	1.9956	6.1904	6.6247	1367
351.5	3.0993	7.3045	7.7479	2051
352.0	3.8120	8.3017	8.9306	2734

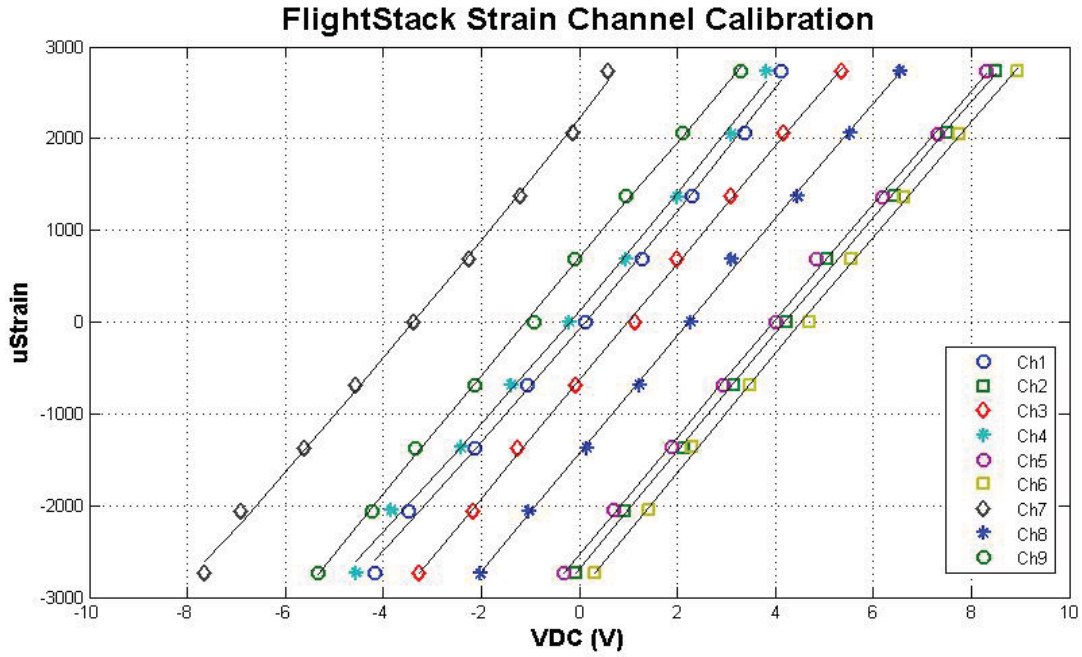

Figure 21: Voltage to Strain Calibration

References

1. Garza, F. and and Morelli, E. *A Collection of Nonlinear Aircraft Simulations in Matlab* . s.l. : NASA, 2003. pp. 45-49. NASA/TM-2003-212145.
2. Owens, D., Cox, D. and Morelli, E. *OwensDevelopment of a Low-Cost Sub-Scale Aircraft for Flight Research: The FASER Project.* s.l. : AIAA, 2006.
3. MathWorks, Inc. xPC Target Selecting Hardware Guide, February 2007 Online only. [Online] 2007. pp. 2-14 - 2-16.
4. Murch, A., Cox, D. and Cunningham, K. *Software Considerations for Subscale Flight Testing of Experimental Control Laws, AIAA paper 2009-2054.* 2009 : AIAA.
5. Strom, T. *Edge 540T Unmanned Aerial Research Vehicle Model Development and Testing.* s.l. : NASA, 2011.
6. Ely, J., et al. *Radiated Emissions From Remote-Controlled Airplane, Measured in a Reverberation Chamber.* s.l. : NASA, 2011. 000000.
7. Oppenheim, A., and Schafer, R. *Discrete-Time Signal Processing*, Prentice-Hall, Inc., 1989. pp. 447-450.
8. Fassios, Spilos F., and Sakellariou, John S. *Fassios,Time-Series Methods for Fault Detection and Identification in Vibrating Structures*, Phil. Trans. R. Soc. , 2007. pp. 365, 421.
9. Wolf, Stanley. *Guide To Electronic Measurements and Laboratory Practice.* Englewood Cliffs, NJ : Prentice-Hall, Inc., 1973. p. 420. 0-13-369587-5.
10. Mathworks, Inc. Xpc Target 4 User's Guide, September 2010 online only revised for version 4.4 release 2010b. [Online] 2010. p.15-28.
11. Vranas, T. Photo on p. 2 used courtesy of Tom Vranas of Vranasphoto.com.

REPORT DOCUMENTATION PAGE

Form Approved
OMB No. 0704-0188

1. REPORT DATE *(DD-MM-YYYY)*	2. REPORT TYPE	3. DATES COVERED *(From - To)*
01- 05 - 2011	Technical Memorandum	

4. TITLE AND SUBTITLE

A Data System for a Rapid Evaluation Class of Subscale Aerial Vehicle

5a. CONTRACT NUMBER

5b. GRANT NUMBER

5c. PROGRAM ELEMENT NUMBER

6. AUTHOR(S)

Hogge, Edward F.; Quach, Cuong C.; Vazquez, Sixto L.; Hill, Boyd L.

5d. PROJECT NUMBER

5e. TASK NUMBER

5f. WORK UNIT NUMBER

534723.02.05.07

7. PERFORMING ORGANIZATION NAME(S) AND ADDRESS(ES)

NASA Langley Research Center
Hampton, VA 23681-2199

8. PERFORMING ORGANIZATION REPORT NUMBER

L-19991

9. SPONSORING/MONITORING AGENCY NAME(S) AND ADDRESS(ES)

National Aeronautics and Space Administration
Washington, DC 20546-0001

10. SPONSOR/MONITOR'S ACRONYM(S)

NASA

11. SPONSOR/MONITOR'S REPORT NUMBER(S)

NASA/TM-2011-217145

12. DISTRIBUTION/AVAILABILITY STATEMENT

Unclassified - Unlimited
Subject Category 06
Availability: NASA CASI (443) 757-5802

13. SUPPLEMENTARY NOTES

14. ABSTRACT

A low cost, rapid evaluation test aircraft is used to develop and test airframe damage diagnosis algorithms at Langley Research Center as part of NASA's Aviations Safety Program. The remotely operated subscale aircraft is instrumented with sensors to monitor structure response during flight. Data is collected for good and compromised airframe configurations to develop data driven models for diagnosing airframe state. This paper describes the data acquisition system (DAS) of the rapid evaluation test aircraft. A PC/104 form factor DAS was developed to allow use of Matlab®, Simulink® simulation code in Langley's existing subscale aircraft flight test infrastructure. The small scale of the test aircraft permitted laboratory testing of the actual flight article under controlled conditions. The low cost and modularity of the DAS permitted adaptation to various flight experiment requirements.

15. SUBJECT TERMS

Flight Instrumentation, Attitude Heading Reference System, Avionics, Data Acquistion System, In-Flight Airframe Measurements, Subscale Test Aircraft, Unmanned Air System, Unmanned Air Vehicle

16. SECURITY CLASSIFICATION OF:			17. LIMITATION OF ABSTRACT	18. NUMBER OF PAGES	19a. NAME OF RESPONSIBLE PERSON
a. REPORT	b. ABSTRACT	c. THIS PAGE			STI Help Desk (email: help@sti.nasa.gov)
					19b. TELEPHONE NUMBER *(Include area code)*
U	U	U	UU	32	(443) 757-5802